THE ASTROPHYSICAL JOURNAL, 186:1171–1178, 1973 December 15

THE COLOR-MAGNITUDE DIAGRAM OF THE METAL-POOR SOUTHERN GLOBULAR CLUSTER NGC 4372

F. D. A. HARTWICK*
University of Victoria

AND

JAMES E. HESSER
Cerro Tololo Inter-American Observatory†
Received 1973 May 16

ABSTRACT

A photometric *UBV* study to $V = 17.2$ of the globular cluster NGC 4372 has revealed: (1) a color-magnitude diagram characteristic of very metal-poor clusters; (2) a large and variable absorption in front of the cluster; and (3) a distance modulus of 13.65 ± 0.20. Attention is drawn to a relatively well populated group of stars lying above the horizontal branch in the color-magnitude diagram.

Subject headings: abundances, stellar — globular clusters — interstellar reddening

I. INTRODUCTION

In spite of the fact that the southern globular cluster NGC 4372 [$\alpha(1950) = 12^{h}23^{m}.0$, $\delta(1950) = -72°24'$; $l^{II} = 301°$, $b^{II} = -10°$] has an unusually low degree of central concentration, which in general facilitates an observational study, no published color-magnitude (C-M) diagram is available for this cluster. In view of the importance of obtaining C-M diagrams for as many of the galactic globular clusters as possible with the ultimate aim of understanding the early evolution of the Galaxy, we obtained photoelectric *UBV* and photographic *B*, *V* photometry of NGC 4372 over a 3-year period when time was available from our metal-rich globular cluster observing program (Hartwick and Hesser 1972). To aid in the disentangling of the complex reddening in the region, additional photometric data for early-type field stars were obtained in the *uvby*–Hβ system. This paper presents the results of these observations.

II. OBSERVATIONS

The photoelectric data obtained for NGC 4372 consist of a sequence of bright secondary standards set up around the cluster on several nights in 1969 and 1970 with the 41-cm and 91-cm telescopes on Cerro Tololo using standard single-channel refrigerated 1P21, *UBV* equipment. These bright stars are identified in figure 1 (plate 5), and their magnitudes, colors, and number of observations are listed in table 1. The standard stars used have been described elsewhere (Hartwick, Hesser, and McClure 1972; Hartwick and Hesser 1972). Median internal standard errors for those stars with multiple observations are: ± 0.007 mag in V, ± 0.004 mag in $(B - V)$, and ± 0.005 mag in $(U - B)$. In addition to the bright stars of table 1, a sequence of fainter stars was observed photoelectrically with the 91-cm and 152-cm telescopes. These stars are also identified in figure 1, and the photometric data are given in table 2.

* Visiting Astronomer, Cerro Tololo Inter-American Observatory.

† Operated by the Association of Universities for Research in Astronomy, Inc., under contract with the National Science Foundation.

TABLE 1

PHOTOELECTRIC OBSERVATIONS OF BRIGHT STARS NEAR NGC 4372

Star	V	$B-V$	$U-B$	n
A..................	6.59	0.00	−0.04	10
B..................	8.90	0.54	+0.05	9
C..................	9.50	1.13	+0.82	6
D..................	9.89	0.58	+0.05	7
E..................	11.26	1.34	+1.09	9
F..................	9.24	0.49	0.00	5
G..................	10.63	0.37	+0.18	1
H..................	10.30	0.42	+0.11	7
I..................	12.10	1.51	...	1
J..................	12.01	0.87	+0.36	8

Median internal standard errors for these observations are: ± 0.02 mag in V and $(B-V)$, and ± 0.03 mag in $(U-B)$.

Photographic plates of NGC 4372 both in V(103aD + GG14) and B(103aO + GG13) were obtained with the f/7.5 camera of the 152-cm telescope. Iris photometry of 338 stars was carried out on two plate pairs. The brighter stars in the inner region (rings 1 and 2 of fig. 2 [plate 6] were measured on a 15-min-exposure plate pair. A larger group of stars including fainter ones were then measured in rings 3 and 4 of figure 2 on a 30-min-exposure plate pair. It was found necessary to apply a small color equation to the raw colors of stars measured on the 15-min plate pair. No corrections were applied to the second group of measurements. The stars are identified in figure 2 and are listed in table 3 according to the ring number shown on the figure. Based on

TABLE 2

OBSERVATIONS OF FAINT SEQUENCE STARS NEAR NGC 4372

Star	V_{pe}	$(B-V)_{pe}$	$(U-B)_{pe}$	n	V_{pg}	$(B-V)_{pg}$
1	12.30	1.76	2.01	3	12.31	1.70
2	12.37	1.78	1.73	5	12.38	1.78
3	12.67	1.36	1.01	7	12.66	1.39
4	12.93	1.00	0.54	5	12.90	0.99
5	13.34	0.89	0.31	4	13.33	0.91
6	13.56	1.27	0.77	2	13.59	1.20
7	14.05	1.31	0.89	2	14.03	1.28
8	14.28	0.66	0.26	5	14.37	0.60
9	14.33	0.82	0.26	4	14.35	0.80
10	14.48	1.41	1.30	3	14.48	1.48
11	14.91	1.85		1	14.89	1.92
12	15.15	0.85	0.23	3	15.18	0.90
13	15.47	0.95		1	15.42	1.00
14	15.57	1.19		1	15.46	1.25
15	15.65	1.12	0.64	2	15.70	1.09
16	15.68	0.66	0.48	2	15.67	0.72
17	15.76	0.53	0.41	1	15.84	0.38
18	15.76	0.71		1	15.74	0.74
19	15.89	0.76	0.44	3	15.90	0.82
20	15.90	0.39	0.27	2	15.91	0.47
21	16.07	1.14		1	16.03	1.10
22	16.11	0.38	0.24	2	16.05	0.42
23	16.16	0.51	0.27	1	16.26	0.41
24	16.26	1.20	1.33::	1	16.23	1.16
25	16.35	0.47	0.41	1	16.40	0.39
26	16.35	0.65	0.47	1	16.50	0.62
27	16.39	1.16	0.07	1	16.40	1.08
28	16.55	1.07	0.41:	1	16.53	1.14
29	16.99	1.25		1	16.90	1.33
30	17.16	1.06		2	17.14	1.10

1973ApJ...186.1171H

TABLE 3

PHOTOGRAPHIC PHOTOMETRY OF PROGRAM STARS

Star	V	B-V	Star	V	B-V	Star	V	B-V	Star	V	B-V	Star	V	B-V
1009	14.41	1.06	2215	13.48	1.16	3092	14.39	1.25	3186	15.25	0.99	4055	14.91	1.20
1010	14.21	1.33	2218	15.24	1.17	3093	13.96	0.91	3189	15.20	1.07	4056	16.02	0.54
1011	14.95	1.17	2228	15.24	1.15	3096	16.27	0.44	3192	16.97	1.15	4058	15.90	0.51
1019	13.64	1.58	2234	14.27	0.97	3097	16.53	1.24	3195	15.21	1.02	4059	16.33	1.15
1024	12.99	1.61	2237	14.55	1.23	3099	16.16	1.24	3199	15.52	0.83	4060	16.58	1.23
1025	15.00	1.20	2254	14.88	1.24	3100	15.36	1.30	3201	16.96	1.09	4061	13.91	1.29
1026	14.62	1.38	2259	15.63	1.10	3101	16.35	0.55	3202	15.37	1.07	4062	13.63	1.57
1029	15.17	1.31	2261	15.56	0.50	3102	16.87	1.14	3204	14.25	1.02	4067	16.31	1.01
1040	15.55	1.09	2662	15.26	1.21	3103	15.07	1.26	3206	16.70	1.10	4069	15.65	1.09
1052	15.41	0.69	2263	15.29	1.51	3104	15.99	0.46	3213	15.73	1.04	4070	15.97	0.45
1054	15.17	1.21	2265	14.17	1.54	3105	14.90	1.06	3217	16.73	1.25	4071	16.31	1.15
1064	15.24	0.61	2268	15.16	1.32	3106	14.69	1.26	3225	14.92	1.05	4072	15.11	1.22
1068	15.33	1.05	2273	15.53	1.15	3107	15.66	1.08	3226	15.94	0.34	4073	12.92	1.61
1072	13.65	1.45	3003	16.98	1.20	3108	15.81	0.90	3230	16.86	1.14	4074	16.36	0.37
1079	14.31	0.92	3004	15.97	0.36	3109	16.99	1.21	3231	15.91	0.39	4075	16.34	1.29
1087	13.76	1.35	3005	16.08	0.42	3112	15.67	0.54	3232	15.62	1.07	4078	16.82	1.41
1088	15.05	1.23	3007	15.16	1.14	3114	16.89	1.17	3234	16.03	1.11	4079	16.06	0.35
1090	15.71	0.55	3010	12.60	1.70	3120	13.83	1.36	3236	16.82	1.16	4081	16.04	0.39
1094	14.82	1.36	3011	15.40	1.05	3121	15.99	1.17	3238	15.71	1.09	4082	15.63	1.18
1097	14.84	1.28	3012	15.74	0.48	3122	15.44	1.21	3246	16.14	1.13	4083	16.44	1.16
1103	15.17	1.19	3015	16.82	1.35	3124	15.70	0.60	3247	16.75	1.18	4086	15.87	0.53
1108	14.05	1.23	3016	16.12	1.21	3125	15.88	0.50	3253	15.30	0.52	4089	16.86	1.30
1110	14.46	1.23	3018	16.63	1.24	3131	15.77	1.29	3254	16.88	1.11	4092	16.21	1.26
1111	15.39	1.14	3019	14.42	1.16	3132	16.76	1.26	3255	15.12	1.11	4094	15.54	1.26
2002	12.57	1.81	3021	16.81	1.09	3133	16.29	1.29	3259	16.59	1.31	4095	15.35	1.17
2005	15.68	0.50	3022	15.97	1.15	3134	14.10	1.31	3260	13.65	1.36	4096	15.75	0.48
2013	14.63	0.95	3023	14.11	1.29	3137	15.94	0.54	3262	15.60	0.31	4097	16.95	1.18
2017	11.92	1.81	3024	15.98	0.49	3138	14.15	1.38	3265	16.34	0.97	4098	16.14	0.40
2020	14.31	1.43	3025	15.48	1.20	3139	16.28	1.17	3266	16.08	0.36	4099	15.96	0.45
2052	15.57	1.19	3026	15.87	1.29	3140	15.30	1.16	3267	16.61	1.13	4101	16.27	1.25
2053	14.48	1.32	3027	16.69	1.23	3142	14.02	1.37	3269	15.69	1.03	4102	16.16	0.58
2059	14.95	1.34	3028	16.57	1.46	3142	16.08	1.36	3271	15.98	0.30	4103	15.23	1.16
2063	12.34	1.60	3029	16.69	1.59	3144	16.25	0.56	4001	15.80	1.29	4104	15.79	1.09
2066	15.30	1.23	3033	12.52	1.75	3146	16.22	0.55	4002	12.23	1.82	4105	15.55	1.16
2082	15.21	1.19	3035	12.62	1.75	3148	16.96	1.23	4004	15.93	1.10	4106	16.12	0.41
2084	14.61	1.33	3037	15.43	1.27	3149	16.55	1.33	4005	14.99	1.14	4108	15.57	1.19
2095	14.86	1.24	3038	16.44	1.08	3151	14.76	1.19	4011	15.28	1.23	4110	14.19	1.25
2102	15.23	1.25	3040	16.26	1.25	3153	16.25	1.17	4012	15.77	1.21	4111	16.25	0.39
2113	15.60	1.07	3041	16.48	1.30	3154	15.64	1.14	4014	15.83	1.08	4112	15.47	0.53
2119	15.55	1.14	3053	13.72	1.35	3156	16.51	1.27	4015	14.34	1.55	4114	15.69	1.35
2121	12.90	1.54	3055	15.12	1.17	3157	16.55	1.16	4017	16.97	1.10	4115	16.11	1.38
2141	15.13	1.24	3057	16.56	1.51	3158	16.02	0.35	4020	16.14	0.39	4116	15.86	1.28
2153	15.68	1.23	3061	15.85	0.65	3160	16.99	1.34	4021	16.30	1.23	4117	13.10	1.50
2154	13.95	1.30	3062	16.79	0.66	3161	16.28	1.23	4025	15.37	1.19	4118	15.28	1.24
2155	12.99	1.46	3063	16.62	0.64	3162	15.55	0.86	4026	15.77	0.60	4119	13.21	1.46
2156	14.63	1.19	3064	16.52	1.45	3164	16.12	0.40	4028	14.79	1.11	4120	16.26	1.31
2157	15.59	0.58	3065	15.94	1.41	3165	16.26	1.22	4030	16.75	1.14	4121	15.68	1.21
2158	15.57	0.68	3067	16.17	1.33	3166	16.48	1.11	4032	16.20	0.50	4124	13.83	1.23
2174	15.32	1.18	3068	14.14	1.27	3168	14.36	1.41	4033	15.94	1.31	4125	16.55	1.18
2181	15.49	0.52	3069	14.17	1.47	3169	16.48	1.28	4034	15.56	1.24	4126	16.73	1.02
2183	14.98	1.28	3072	15.85	1.27	3170	14.18	1.23	4035	14.96	1.25	4127	15.98	0.33
2184	15.44	0.69	3073	14.62	0.80	3173	16.10	1.16	4036	16.89	1.19	4128	15.26	0.47
2185	12.99	1.35	3074	16.77	1.12	3174	15.81	1.18	4038	17.01	1.25	4132	16.79	1.20
2187	12.51	1.50	3075	15.59	1.27	3176	16.08	1.30	4044	15.85	1.26	4133	13.77	1.22
2188	15.53	0.46	3076	16.33	1.39	3177	13.87	1.21	4046	16.69	1.21	4134	13.47	1.24
2193	15.27	0.51	3079	16.63	1.32	3178	15.19	1.37	4049	16.04	1.23	4136	15.88	1.58
2196	15.70	0.51	3085	14.50	1.18	3180	14.29	0.88	4050	16.76	1.28	4137	15.78	0.37
2208	15.67	1.08	3088	14.43	1.19	3182	16.81	1.10	4052	16.66	0.34	4138	15.66	1.10
2209	14.81	1.20	3089	15.16	1.51	3183	15.53	1.09	4053	15.93	1.19	4142	16.09	1.44
2214	15.31	0.56	3091	16.32	0.50	3184	16.26	1.29	4054	16.26	0.34	4143	15.26	1.10

TABLE 3—*Continued*

Star	V	B-V	Star	V	B-V	Star	V	B-V	Star	V	B-V	Star	V	B-V
4146	16.29	0.83	4161	16.71	1.16	4173	15.70	0.43	4195	16.77	1.18	4210	15.46	1.10
4148	15.80	0.41	4163	15.88	1.07	4176	16.68	1.24	4196	16.23	0.39	4212	15.44	1.37
4149	15.47	0.82	4164	15.90	1.12	4178	15.53	0.44	4197	15.89	0.26	4214	16.42	1.11
4150	15.28	1.15	4166	15.88	0.41	4182	16.10	0.33	4200	16.02	0.42	4221	16.38	1.11
4152	16.80	1.21	4167	14.69	0.92	4183	16.86	1.10	4201	15.54	0.40	4222	15.37	0.34
4154	16.77	1.51	4169	15.77	1.11	4184	16.01	0.40	4202	16.03	0.96	4225	16.35	1.11
4155	15.78	0.38	4171	15.79	1.15	4188	16.68	1.30	4208	13.85	0.79			
4158	15.97	1.22	4172	14.43	0.98	4194	16.21	1.72	4209	16.73	1.24			

previous work we estimate the median internal standard error of a single observation in table 3 to be ± 0.02 mag in V and ± 0.03 mag in $(B - V)$. As unraveling the complex differential reddening (§ III) will require higher precision than we feel can be obtained by classical photographic photometry (even of several plate pairs), the only advantage to be accrued from additional photographic photometry would be the removal of the occasional accidental errors that go undetected when only one plate pair is measured. The agreement from stars in common on the bright and faint plate pairs measured was good, and we have chosen to present data from only one plate pair until such time as it becomes clear that the cluster deserves to be studied with greater precision by other techniques.

III. RESULTS

The color-magnitude diagram for NGC 4372 is shown in figure 3, where we have plotted the photoelectric results from table 2 as plus signs, the photographic results

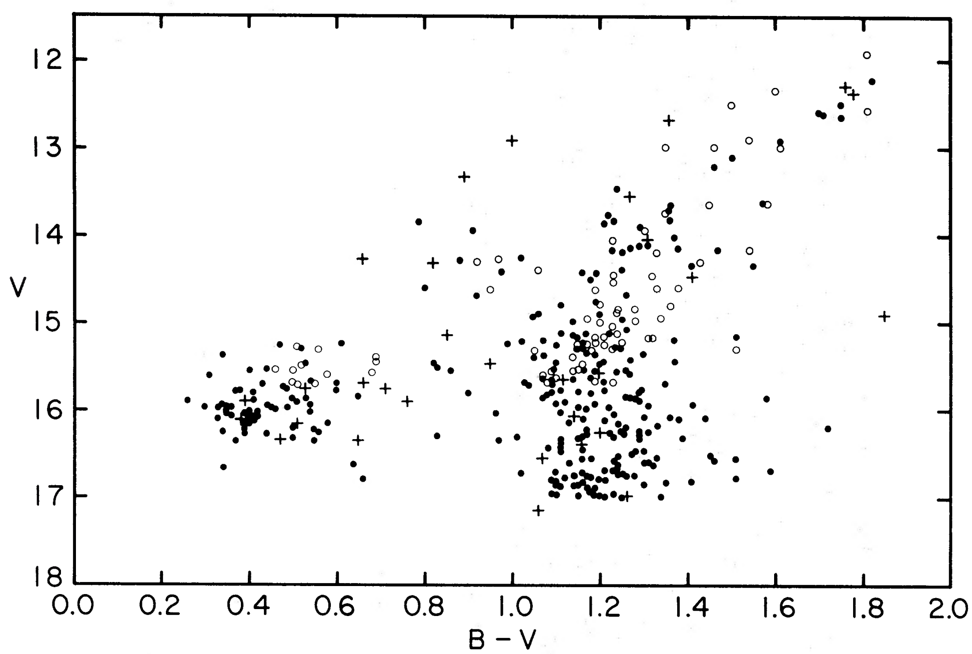

FIG. 3.—The color-magnitude diagram for NGC 4372. Plus signs represent the photoelectric observations of table 2; open circles, the 1000 and 2000 stars of table 3; filled circles, the 3000 and 4000 stars of table 3.

for rings 1 and 2 of figure 2 as open circles, and the results for rings 3 and 4 as closed circles. In spite of the large scatter, the diagram shows a relatively steep giant branch and a blue horizontal branch, which are both characteristics of a metal-poor globular cluster.

Before comparing figure 3 with the C-M diagrams of other globular clusters, we shall estimate the reddening of NGC 4372. Figure 4 shows the two-color diagram for the stars in table 2 after correcting for a reddening of $E(B-V) = 0.42$–0.48. The five reddest stars in figure 4 have had their reddening removed following the procedure of Hartwick and McClure (1972), which allows for the change in slope of the reddening trajectory as a function of intrinsic color. It is apparent from figure 4 that NGC 4372 is differentially reddened by approximately 0.06 mag. This result would account for part of the large scatter that we noted previously in figure 3. We attempted to map the differential reddening by plotting C-M diagrams for small regions of the cluster separately and from star counts. No systematic trends were obvious, so we conclude that the absorption is very patchy over the area studied.

As shown by Crawford and Barnes (1969), *uvby*–Hβ photometry (Strömgren 1966) of field B, A, and F stars can provide reliable reddening estimates for cluster fields. In 1972 we observed 32 stars from the HD catalog with the 61-cm Lowell-Tololo telescope equipped with a standard 1P21 photometer and CTIO filter set number 3. Five nights out of a much more extensive program were used to obtain the data for NGC 4372, and mean extinction and transformation coefficients determined from many nights were used for the reductions. The results are presented in table 4; the median internal standard errors of an individual measurement entering into the means, as determined from those stars with multiple observations, are 0.010, 0.004, 0.008, 0.012, and 0.010 mag for y, $b-y$, m_1, c_1, and β, respectively. The y-magnitudes of table 4 were obtained by linearly transforming to the V-magnitude of the *UBV* system. Reddening was determined individually using the preliminary relations of Crawford (1970). Similarly, the preliminary absolute-magnitude calibrations (Crawford 1972) were applied wherever possible, and allowances for evolutionary

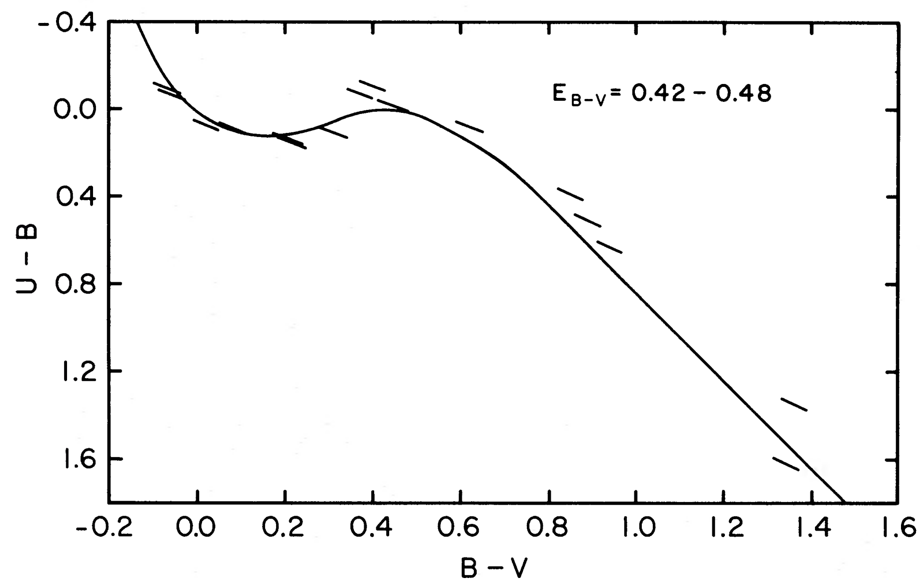

FIG. 4.—The two-color diagram for the photoelectric observations of table 2 corrected for a reddening of $E(B-V) = 0.42$ to 0.48.

TABLE 4

uvby AND Hβ PHOTOMETRY OF B, A AND F STARS NEAR NGC 4372

Star (HD)	y	b-y	m_1	c_1	β	n	E(B-V)	M_V	r(pc)
106676	6.222	-0.015	0.144	1.000	2.866	3	0.05	1.10	98
106759	7.825	0.242	0.113	1.093	2.839	3	0.24	0.54	204
106782	8.648	0.105	0.052	0.428	2.708	3	0.25	-0.70	520
106830	8.390	0.327	0.094	1.092	2.785	3	0.29	0.02	309
106882	9.057	0.164	0.100	1.242	2.879	1	0.19	-0.31	565
107316	9.022	0.210	0.018	0.439	2.707	3	0.39	-0.70	499
107483	9.297	0.177	0.108	0.953	2.873	2	0.17	1.98	229
107547*	6.771	0.076	0.194	1.025	2.866	3	0.02	1.51	110
107875	9.652	0.175	0.041	0.842	2.774	3	0.29	0.25	499
107947	6.610	-0.007	0.163	0.958	2.902	3	0.02	1.40:	107
107983	8.082	0.128	0.078	0.908	2.828	3	0.22	0.72	217
108098	9.724	0.263	0.161	1.014	2.844	3	0.25	1.26	343
108297*	8.718	0.170	0.030	0.537	2.716	3	0.32	-1.56	712
108343	8.025	0.129	0.195	0.824	2.816	3	0.01	2.60	121
108419	9.636	0.366	0.185	0.436	2.626	3	0.03	3.30	177
108734	9.308	0.125	0.097	1.191	2.834	3	0.42	-0.19	436
108735	7.086	0.147	0.174	0.860	2.792	3	0.07	1.96	96
108751	8.748	0.222	0.160	0.752	2.757	1	0.06	2.42	169
108764	9.949	0.276	0.065	1.110	2.865	2	0.32	0.67	597
108792†	7.494	0.106	0.075	1.012	2.786	2	-0.02	0.70	313
109010	9.966	0.173	0.142	0.933	2.913	2	0.27	1.50:	336:
109026	3.839	-0.076	0.111	0.359	2.687	4	0.01	-1.10	96
109050	10.124	0.141	0.094	0.754	2.878	2	0.26	1.20	422
109066	9.539	0.253	0.017	0.710	2.764	2	0.42	0.11	421
109067	7.765	0.253	0.166	0.532	2.685	3	-0.01	2.99	92
109082	8.070	0.184	0.051	0.971	2.794	2	0.29	0.43	223
109183	9.135	0.135	0.101	1.009	2.905	3	0.21	1.45:	254:
109211	8.932	0.168	0.177	0.922	2.871	2	0.14	1.99	200
109234	9.608	0.206	0.046	0.901	2.821	2	0.33	0.68	381
109357	9.872	0.269	0.101	1.032	2.768	2	0.19	0.30	628
109399	7.627	0.061	0.028	-0.044	2.569	2	0.24	-4.0 :	1450:
109412	9.728	0.356	0.161	0.799	2.714	3	0.21	1.33	355

* Noted at the telescope as a double star.

† Identification uncertain.

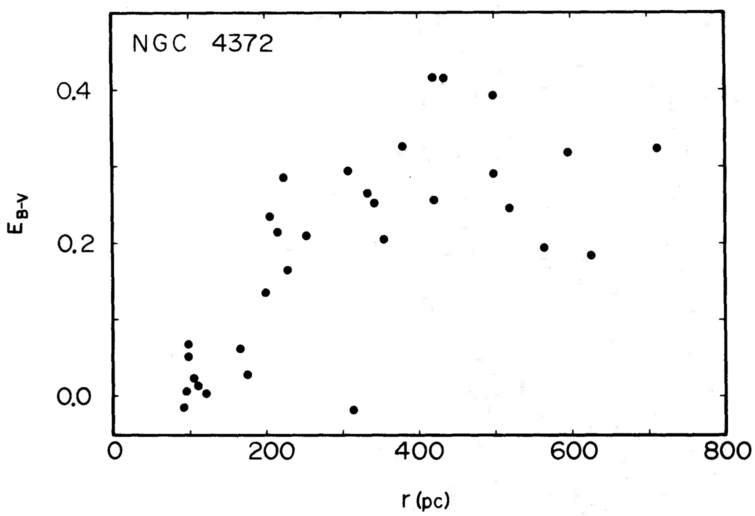

FIG. 5.—A plot of reddening against distance derived from *uvby*–Hβ photometry (table 4) for early-type field stars in the vicinity of NGC 4372. Beyond 250 pc, a leveling off and a large non-uniformity of the reddening are apparent.

effects in the A and F stars were included. Adopting $A_V/E(B - V) = 3.2$, the distances were estimated and the resultant plot of $E(B - V)$ versus distance is shown in figure 5. If, following the discussion of Arp (1965), an absorption layer thickness of 100 pc is assumed, the line of sight to NGC 4372 intersects the layer at a distance of 570 pc, well beyond the point (250 pc) where a leveling off of the reddening versus distance relation is evident in figure 4. The data of figure 4 and table 5 clearly demonstrate the nonuniform nature of the reddening in the vicinity of NGC 4372. From the 18 stars with $r \geq 250$ pc, an average reddening of 0.26 mag is found, but a scatter of 0.10 mag in the individual values is present. Although the *UBV* data indicate that the more immediate vicinity of the cluster (not sampled in the *uvby*–Hβ photometry due to the lack of bright, early-type stars) suffers from reddening that is slightly higher than average for this field, the *uvby*-Hβ results seem to be consistent with the *UBV* analysis presented above.

As a final check on our reddening determination, as well as to enable an estimate of the distance modulus to be made, we superposed our figure 3 on those of two well-studied clusters with similar C-M diagrams. As a result of the comparison with M92 (Sandage and Walker 1966; Sandage 1970) we find $E(B - V)_{4372} = 0.45$ and $(m - M)_{0,4372} = 13.5$ assuming that $E(B - V)_{\rm M92} = 0.02$ and $(m - M)_{0,\rm M92} = 14.56$ (Sandage 1970). Using M2 (Arp 1955) as the standard cluster,[1] we find $E(B - V)_{4372} = 0.40$ and $(m - M)_{0,4372} = 13.8$ with $E(B - V)_{\rm M2} = 0.05$ and $(m - M)_{0,\rm M2} = 15.6$ from Arp (1955). We should emphasize that the features of figure 3 are very similar to those in the C-M diagrams for both M92 and M2.

Many years ago Deutsch (Kinman 1959) classified several globular clusters into three groups based on the strength of the metal lines in the spectra of individual giant-star members. On this system M92 was classified as type C (extremely poor) and M2 as type B (moderately metal poor). Kinman (1959) applied Deutsch's scheme to several southern globular clusters, among them NGC 4372, which he classified as type B. The results of this paper are consistent with Kinman's classification.

Before concluding, we wish to draw attention to a possible group of stars at $V \simeq 14.3$, $B - V \simeq 0.92$. These stars occupy the same region of the C-M diagram as certain stars isolated by Strom *et al.* (1970) and by Zinn, Newell, and Gibson (1972) in a number of other globular clusters. Should further study show that these stars are radial-velocity members, then NGC 4372 would be unusual in having so many of these stars.

IV. SUMMARY

From our photometric investigation of NGC 4372 in the *UBV* and *uvby*–Hβ systems, we conclude that: (1) The C-M diagram of the cluster is characteristic of very metal-poor clusters, a conclusion consistent with Kinman's (1959) spectroscopic classification. (2) The cluster is heavily reddened, and this reddening is patchy over an 8′ region centered on the cluster. We find $E(B - V) = 0.42$–0.48. (3) The distance modulus of NGC 4372 is approximately $(m - M) = 13.65 \pm 0.20$. (4) A group of stars at $V \simeq 14.3$ and $(B - V) \simeq 0.92$ is apparently analogous to the distinct group of stars isolated in other clusters by Zinn *et al.* (1972). If future radial-velocity measurements show that these stars are members, then NGC 4372 would appear to be distinguished in having a populous group of supra-horizontal-branch stars.

We wish to thank Srta. Laura Vega and Mrs. Jeannette Barnes for their invaluable aid in the data reductions, and one of us (F. D. A. H.) wishes to acknowledge financial support from the National Research Council of Canada and the University of Victoria.

[1] The transformation from the $m_{\rm pg}$, $m_{\rm pv}$ system to the *B*, *V* system for M2 was achieved using the relation given by Arp and Melbourne (1959).

REFERENCES

Arp, H. C. 1955, *A.J.*, **60**, 317.
———. 1965, *Ap. J.*, **141**, 43.
Arp, H. C., and Melbourne, W. G. 1959, *A.J.*, **64**, 28.
Crawford, D. L. 1970, in *Stellar Rotation*, ed. A. Slettebak (Dordrecht: Reidel), p. 204.
———. 1972, IAU Symposium 54, Geneva.
Crawford, D. L., and Barnes, J. V. 1969, *A.J.*, **74**, 1008.
Hartwick, F. D. A., and Hesser, J. E. 1972, *Ap. J.*, **175**, 77.
Hartwick, F. D. A., Hesser, J. E., and McClure, R. D. 1972, *Ap. J.*, **174**, 557.
Hartwick, F. D. A., and McClure, R. D. 1972, *Pub. A.S.P.*, **84**, 288.
Kinman, T. D. 1959, *M.N.R.A.S.*, **119**, 538.
Sandage, A. 1970, *Ap. J.*, **162**, 841.
Sandage, A., and Walker, M. F. 1966, *Ap. J.*, **143**, 313.
Strom, S. E., Strom, K. M., Rood, R. T., and Iben, I. 1970, *Astr. and Ap.*, **8**, 243.
Strömgren, B. 1966, *Ann. Rev. Astr. and Ap.*, **4**, 433.
Zinn, R. J., Newell, E. B., and Gibson, J. B. 1972, *Astr. and Ap.*, **18**, 390.

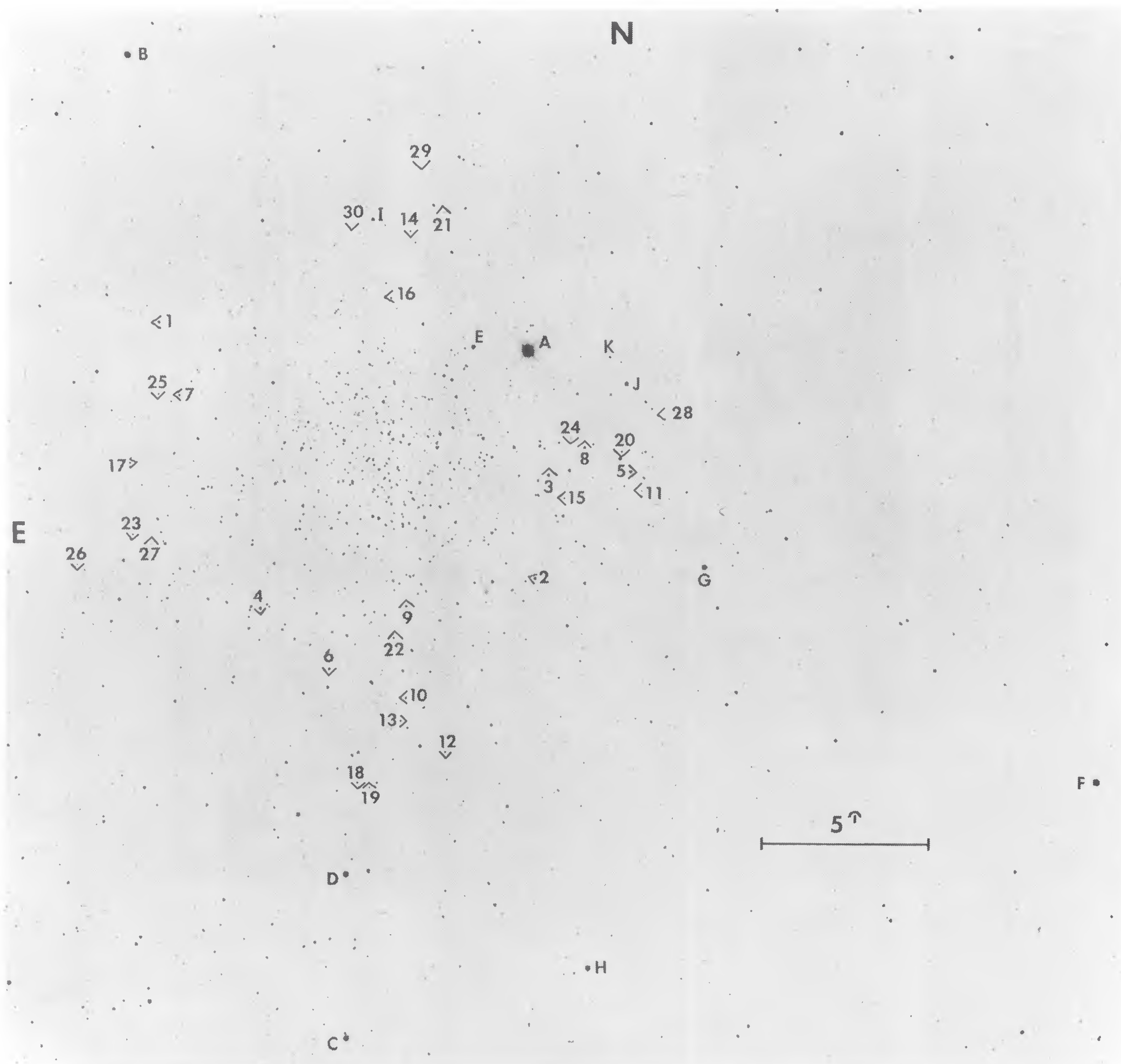

FIG. 1.—Reproduction of a 15-min *B* (103aO + GG13) plate taken with the 152-cm telescope showing the bright secondary standard stars (*lettered*) and the faint sequence stars (*numbered*) in the vicinity of NGC 4372 that were measured photoelectrically.

HARTWICK AND HESSER (*see* page 1171)

PLATE 6

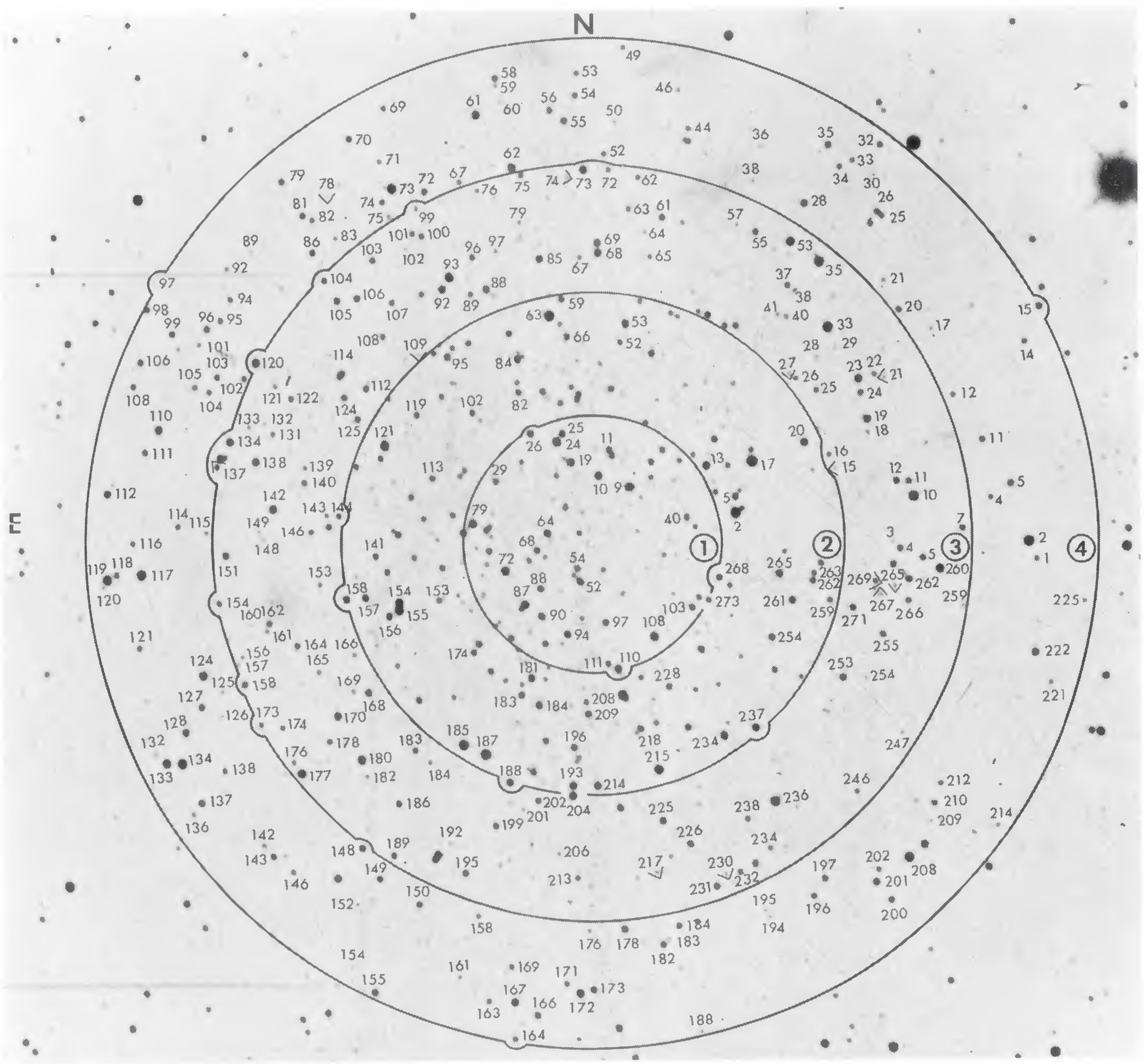

FIG. 2.—Reproduction of the same plate as fig. 1 showing the photographically observed stars. The circles have radii of 1′, 2′, 3′, and 4′.

HARTWICK AND HESSER (*see* page 1172)